UNIVERSITY OF OKLAHOMA

GRADUATE COLLEGE

MEASUREMENT AND ANALYSIS OF OIL-GAS DIFFUSION AT RESERVOIR CONDITIONS: APPLICATION TO HUFF-N-PUFF EOR IN UNCONVENTIONAL RESERVOIRS

A THESIS

SUBMITTED TO THE GRADUATE FACULTY

in partial fulfillment of the requirements for the

Degree of

MASTER OF SCIENCE

By

SANCHAY MUKHERJEE
Norman, Oklahoma
2020

MEASUREMENT AND ANALYSIS OF OIL-GAS DIFFUSION AT RESERVOIR CONDITIONS: APPLICATION TO HUFF-N-PUFF EOR IN UNCONVENTIONAL RESERVOIRS

A THESIS APPROVED FOR THE
MEWBOURNE SCHOOL OF PETROLEUM AND GEOLOGICAL ENGINEERING

BY THE COMMITTEE CONSISTING OF

Dr. Chandra S. Rai, Chair

Dr. Carl H. Sondergeld

Dr. Deepak Devegowda

Dedicated to

“My Professors, Family and Friends”

Acknowledgements

I would like to thank my advisors, Dr. Chandra Rai and Dr. Carl Sondergeld for giving me this opportunity to pursue research under their guidance. Their support and motivation have helped me grow professionally and personally. I am thankful to Dr. Deepak Devegowda for his valuable inputs towards my research and academics.

I would also like to thank Dr. Son Dang, Dr. Ishank Gupta and Dr. Ali Tinni for their mentorship and for helping me become a better researcher. They have inspired me to work hard and take risks. I am thankful to Dr. Curtis, Mikki, Gary, Jeremy and my friends at IC^3 for their support, friendship and care.

Finally, I would like to express gratitude to my parents and family for believing in my dreams and for their unconditional love. Special shoutout to my extended family in Oklahoma for all the support and encouragement. Payton, Nachiket, DSD, Rohan, Ashutosh and Karthika; my OU journey would not have been fun without you guys.

Table of Contents

List of Figures

List of Tables

Abstract

Due to the extremely low permeability and high depletion rate, primary recovery from unconventional reservoirs is generally low. Huff-n-Puff has proved to be a successful EOR technique in tight formations, such as the Eagle Ford. However, the underlying transport mechanism remains poorly understood. Recent studies show oil-gas diffusion is a key factor in huff-n-puff EOR. Due to concentration gradients, injected gas molecules diffuse into *in-situ* oil causing it to swell and consequently to be expelled out of the nanopores into the micro- and macro-fractures.

We have designed an experiment with a high-pressure, high-temperature cell having observation windows for the measurement of oil swelling and diffusivity. The measurements have been done on Wolfcamp A oil (API-32), Meramec oil (API-43) and Eagle Ford oil (API-53) with 3 different gas mixtures of methane – ethane, at a temperature of 175°F to evaluate the impact of injection pressure (above and below Minimum Miscibility Pressure-MMP), injectate gas composition, API gravity and viscosity of oil on oil-gas diffusivity.

The results show that the diffusivity of injectate gas into the oil phase as a function of pressure and increases to maximum at MMP, beyond which it decreases. Enrichment of the injection gas increases the oil-gas diffusivity at the same pressure. Regardless of injection pressure, for the gas mixture C1/C2 (72/28 mole%) the diffusion coefficient varies between 10^{-11} m^2/s to 10^{-10} m^2/s for Wolfcamp A oil; 10^{-10} m^2/s to 10^{-9} m^2/s for Meramec oil and 10^{-9} m^2/s to 10^{-8} m^2/s for Eagle Ford oil.

Tight reservoirs generally have a high matrix tortuosity, which impacts the diffusion efficiency in the porous media. Using tortuosity values available in the literature and diffusivities of oil gas systems measured in this study, we estimate that the injected gas can only travel 0.2-0.9 ft away from the fracture-faces during 6 months of gas injection. Low tortuosity and high diffusion rates favor economic recoveries. This study highlights the importance of stimulated reservoir area (SRA) characterization, nanoporous tortuosity and diffusivity measurements in optimizing huff-n-puff recovery in shales.

Chapter 1: Introduction

In the last decade, production from the low permeability, liquid rich unconventional reservoirs has increased to more than 8 MSTB/day in U.S, accounting for 65% of total oil production in the U.S (EIA, 2019). The increase in recovery from these reservoirs has been due to the improvements in horizontal well technology and multistage fracturing. Although these wells may start to produce at high rates initially, the rates drop off quickly (Mobilia et al., 2016, **Figure 1**) leading to low recovery factors in the range of 3 – 10 % of original hydrocarbons in place (Hoffman and Evans, 2016). This quick decline in production rate is due to the fast depletion in natural fractures and low flow of fluids from the rock matrix (Yu et al., 2014).

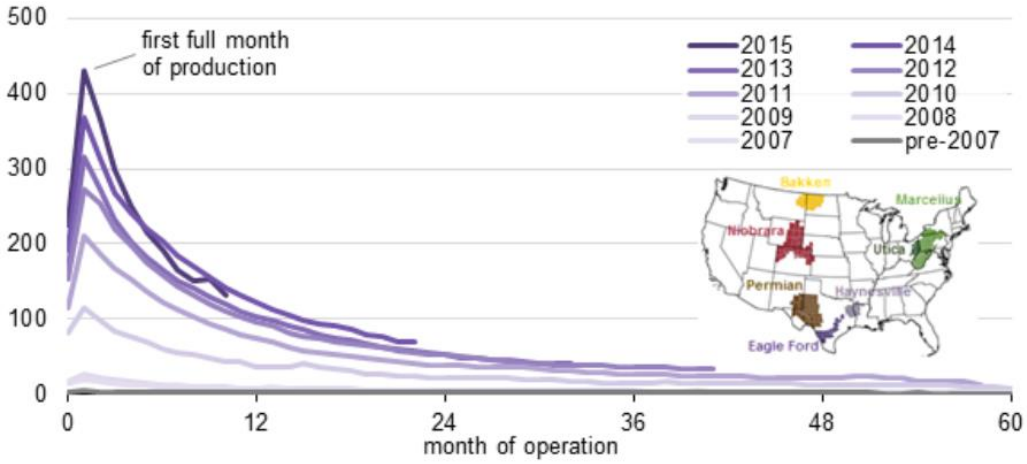

Figure 1. Average oil production per well in the Eagle Ford region. The production from the unconventional wells start at a higher rate which drops off quickly leading to low recovery factors (Mobilia et al., 2016).

As a solution, enhanced oil recovery techniques such as infill drilling, gas injection, surfactant and water flooding were introduced, which depend on the physical, chemical and biological alteration of fluid and/or rock properties to improve oil recovery. Amongst the EOR techniques, gas injection is the most recommended technique for unconventional reservoirs (Nour et al., 2015). Further gas

injection can be of two types; gas flooding and cyclic gas injection or huff-n-puff. In gas flooding technique, the oil reservoirs already waterflooded are injected with hydrocarbon or non-hydrocarbon gases to extract the residual oil (Russel and Dindoruk, 2013). This technique is inefficient for unconventional reservoirs since unlike the conventional reservoirs, the fracture network in tight reservoirs is complex which leads to gas channeling, affecting oil displacement (Wang and Li, 2019). Huff-n-Puff involves the injection of gas into the reservoir (huff phase) followed by soaking and production oil (puff phase) from the same well, and is a popular and highly efficient EOR technique in tight reservoirs (Thomas and Monger, 2007). Recently, Nagarajan et al., 2020 also demonstrated the efficiency of this technique in a two well (vertical injector and horizontal producer) Bakken field test. Table 1 lists some of the pilot tests carried out in the Bakken and Eagle Ford formations (Wang et al., 2017).

No	Operator	Formation	State	Year	Fluid	Type
1	EOG	Bakken	ND, US	2008	CO_2	Huff-n-puff
2	–	Bakken	MT, US	2009	CO_2	Huff-n-puff
3	EOG	Bakken	ND, US	2012	Water	Huff-n-puff
4	EOG	Bakken	ND, US	2012–2013	Water	Flooding
5	EOG	Bakken	ND, US	2014	Natural gas	Flooding
6	Whiting	Bakken	ND, US	2014	CO_2	Huff-n-puff vertical well
7	–	Bakken	MT, US	2014	Water	Flooding
8	Lightstream Resources	Bakken	SK, CA	2011	Natural gas	Flooding
9	Crescent Point Energy	Bakken	SK, CA	2006–2011	Water	Flooding
10	EOG	Eagle Ford	TX, US	2013–2015	Natural gas	Flooding

Table 1. Summary of EOR pilot tests in Bakken and Eagle ford formations (Modified after Wang et al., 2017)

The successful pilot tests in Eagle Ford with natural gas huff-n-puff have proven the effectiveness of this technique (**Figure 2**). The EOR process started with a charging cycle of 6-months injection, the next two cycles had 2.5 months of injection, followed by shorter injection cycles. From EOG

reports in 2016, the process can recover 30 to 70 percent of original estimated ultimate recovery (EUR) (Hoffman, 2018).

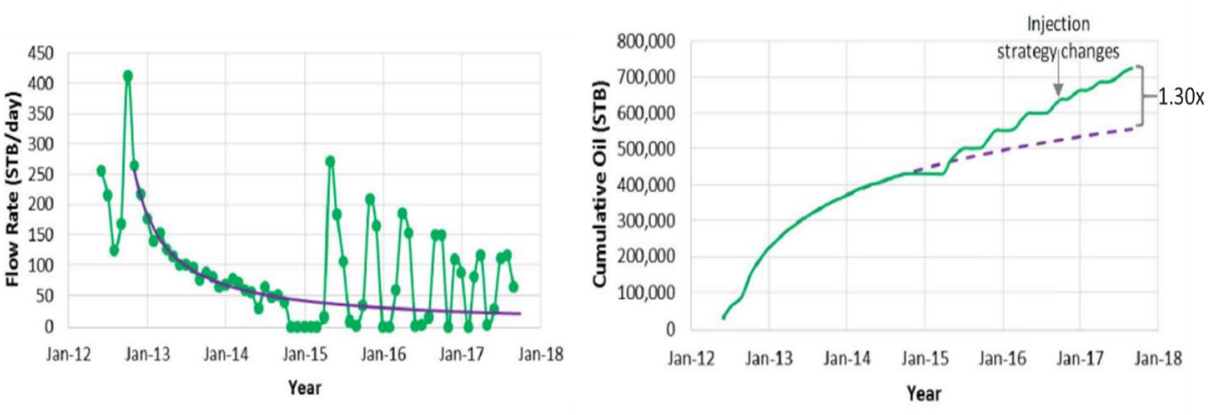

Figure 2. Incremental and cumulative production for the successful pilot test in Eagle Ford formation (Hoffman, 2018). The Huff-n-Puff technique can recover additional 30 % of original EUR in comparison to the predicted recovery.

An effective and economical project depends on the understanding of gas transportation during both injection and flow-back. The increase in recovery from reservoirs like Eagle Ford and Bakken was noted (Wang et al., 2010) and recent studies (Tovar et al., 2018; Li et al., 2016, and Dang, 2019) investigated the transport mechanisms for the enhanced recovery. Recent modelling and theoretical investigations have shown that diffusion could be one of dominant transport mechanisms responsible for fluid flow in low permeability shales.

The displacement of one fluid by another miscible fluid in a porous medium can be represented by Eq. 1 (Perkins et al., 1965). D_o is the bulk diffusion coefficient (cm^2/s). FØ is the matrix tortuosity, v is average displacement velocity, governed by matrix permeability, (cm/sec), d_p is the particle diameter-controlling pore-throat size (cm) and σ is a measure of media heterogeneity. In this equation, the first term is governed by diffusion rate. The second term, which represents advection or mechanical mixing, is dominantly controlled by permeability and capillary pressure in the

porous media. In conventional rocks, due to high porosity and permeability, advection dominates the mass transport mechanism. Whereas, diffusion overpowers the role of advection in tight rocks as the product of permeability and pore-throat in this case reduces by 6 to 9 orders of magnitude as compared to conventional rocks.

$$Dispersion\ Coefficient = \frac{D_o}{F\emptyset} + 0.5vd_p\sigma \quad (1)$$

Li et al. (2019) illustrated the significance of molecular diffusion on fluid sweep volume and cumulative recovery during CO_2 Huff-n-Puff EOR in shale oil reservoirs in a numerical simulation study. Different cases of simulation were created using four values of diffusion coefficients (0 – 2.12 x 10^{-9} m^2/s). As shown in **Figure 3**, both sweep volume percentage and cumulative oil recovery increased with higher diffusion coefficients. With increasing diffusion coefficients, a larger volume of CO_2 is able to penetrate deeper into the rock matrix, leading to high recovery.

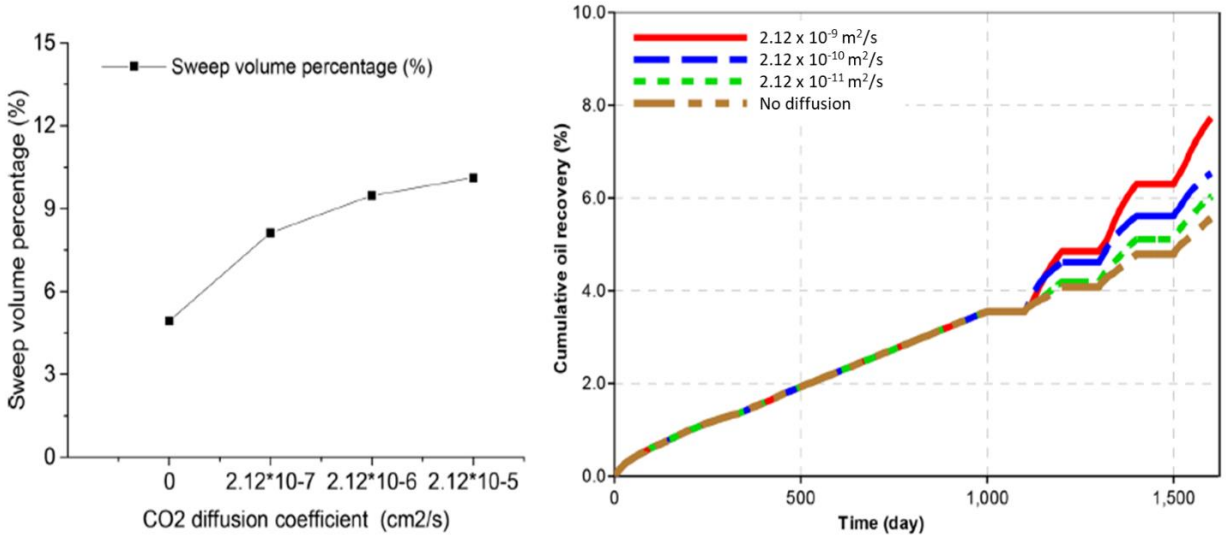

(a) **(b)**

Figure 3. Effect of CO_2 diffusion coefficient on (a) sweep volume percentage and (b) cumulative oil recovery. Increasing the diffusion coefficient results in more oil being produced (Modified after Li et al., 2019).

Production modelling results by Cronin et al.(2018) also emphasize the dominance of diffusion as a transport mechanism for enhanced recovery. Four proxy models are simulated to study the impact of effective diffusion coefficients on the recovery factors and incremental flowrates (**Figure 4**). With increasing diffusion coefficient, the Ultimate Recovery Factor (URF) increases. The depletion by diffusion is also similar to the characteristic recovery profile of tight reservoirs; high initial production followed by sharp decline in rates.

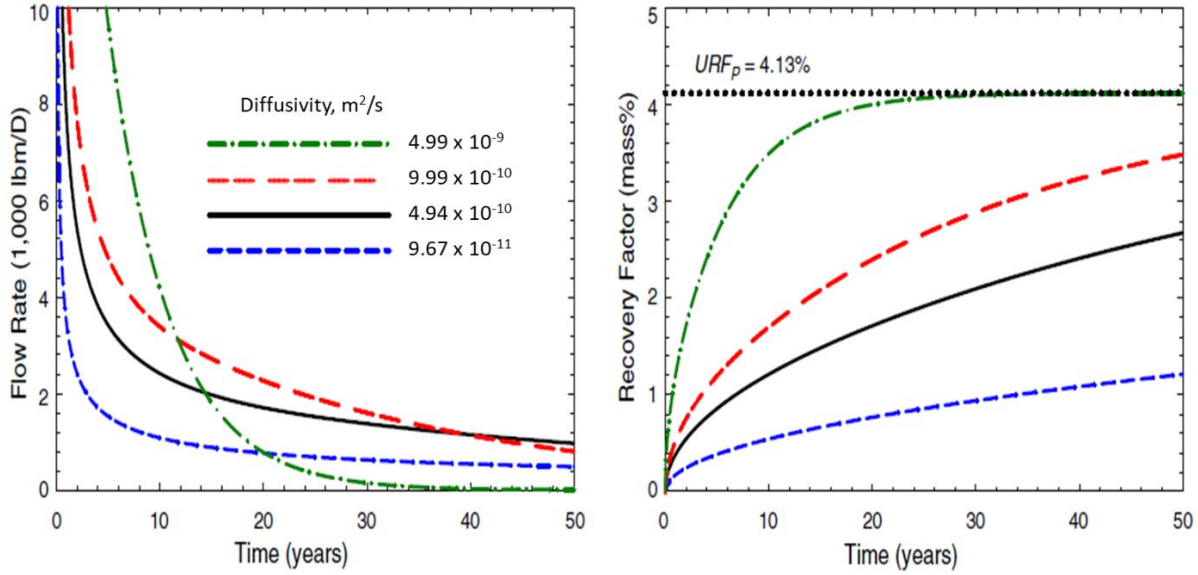

(a) **(b)**

Figure 4. (a) Flow rate and (b) recovery factors for 4 models with different values of effective diffusion coefficients, maintaining all other parameters constant. The model with the highest diffusion coefficient results in highest Ultimate Recovery Factor (URF) in a time span of 50 years, showing the dominance of diffusion in transport of fluids (Modified after Cronin et al., 2018).

Many experimental studies (Hawthorne et al., 2013; Gamadi et al., 2014; Hoteit and Faroozabadi, 2009, and Amann-Hildebrand et al., 2012) have shown the positive effect of diffusion as a recovery mechanism, particularly for fractured reservoirs with low oil and gas permeability. Recently, Dang (2019) performed Huff-n-Puff experiments on an Eagle Ford sample and monitored the recovery

in real time using NMR (**Figure 5**). In this experiment, during both the injection (huff) and production (puff) phases the recovery trend increased. It is known that the recovery during the drawdown phase with a positive pressure gradient towards fracture face, advection dominates the transport mechanism. However, the recovery observed during the injection and soaking phase, with negative or zero pressure gradient should be due to the diffusion of oil and gas. Since during production both advection and diffusion contribute to the recovery and the resulting trend in the experiment is similar for both production and injection phases; it indicates that diffusion is the dominating phenomena for the unconventional tight shales.

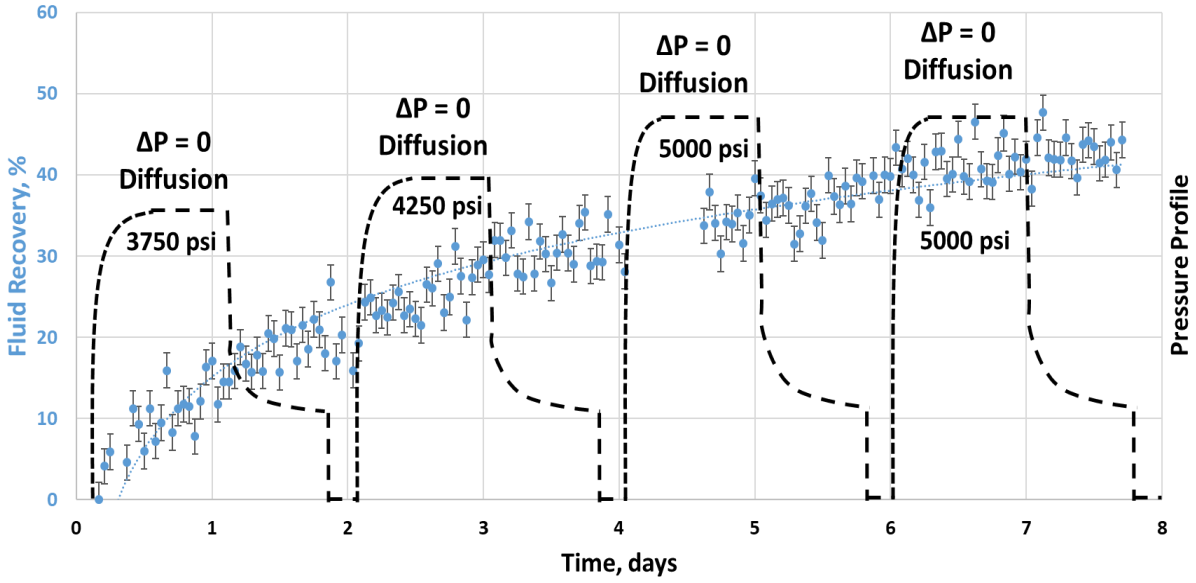

Figure 5. Experimental observation of dominance of diffusion as a transport parameter using NMR real time monitoring of a Huff-n-Puff experiment. The similar recovery trends during both injection and production phases emphasize the significance of diffusion in rocks (Dang, 2019)

Empirically, the molecular diffusion of gas in oil phase could be computed using the Sigmund correlation (1976). The study measured the reduced densities of oil-gas mixtures to formulate a correlation for prediction of diffusion coefficient. Most of the experimental data used to develop

this correlation was measured at atmospheric conditions, which is inappropriate for a subsurface reservoir. Due to the experimental conditions, the predicted diffusion coefficients of gases in liquid hydrocarbons at high pressures by the Sigmund correlation are 80% to 100% higher than reported measured values (Riazi and Whitson (1993)). Denoyelle and Bardon (1983) measured diffusion coefficients for CO_2 in oil at reservoir conditions and reported values 5-10 times lower as compared to those measured using the Sigmund correlation concluding that diffusion coefficients measured at atmospheric conditions are not representative of diffusion coefficients at reservoir conditions.

Riazi (1996) developed a semi-analytical method to predict mass transfer rate due to diffusion between gas and liquid phase under high pressure and constant temperature system. Based on the semi-analytical method, Zhang et al. (2000) developed the pressure-decay method to determine diffusion coefficient of gases in oil phase at static conditions using a PVT cell. Guo et al., (2009) developed another technique to evaluate diffusion coefficient by monitoring pressure profile during oil-gas molecular interaction in a closed cell. These experiments were based on simplistic assumptions, and especially, a constant pressure was not maintained throughout the duration of the experiment. Dang et al., (2020) utilized the Nuclear Magnetic Resonance (NMR) technique to evaluate diffusion coefficient at high pressure conditions (**Figure 6**). The NMR method uses a Daedalus® cell, made of NMR transparent ZrO2; the cell can be operated up to 10,000 psi internal pressure. NMR 1-D gradient profiles are continuously acquired using an Oxford 2MHz GeoSpec™ spectrometer with Green Imaging acquisition and processing software. Typical experiments are performed for 8 days to monitor the dynamic change of hydrogen index (HI) profiles across the oil-gas interface during the diffusion process. This allows extraction of bulk diffusion parameters by directly calculating the concentration of the injectate in the liquid phase. However, due to

experimental limitation, the tests could only be performed at 95°F. The study also showed that the diffusion rate of gas in oil decreases as a function of time. This can be considered as an experimental artifact. While Fick's Law was solved for infinite boundary condition, the test cell has limited volume. As soon as the first gas molecule travelling toward the oil phase approaches the end of the cell, the diffusion rate would be reduced.

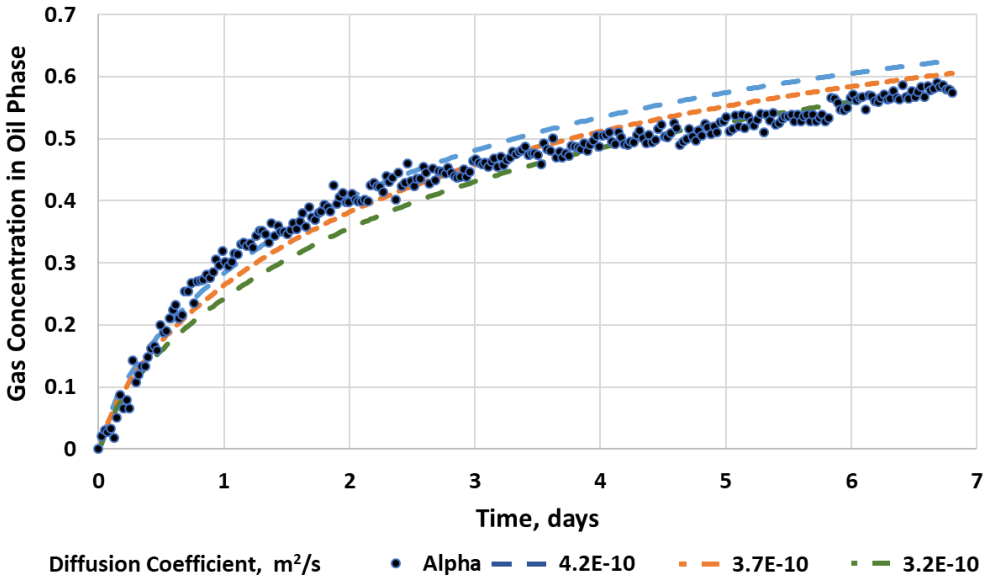

Figure 6. Fitting results for different diffusion coefficients using the relative methane concentration profile. Alpha represents the measured values of gas concentration in oil phase. The whole profile over 8 days can be fit with diffusion coefficients ranging from 3.2×10^{-10} to 4.2×10^{-10} m^2/s; however, it is clear that the diffusion rate decreases as a function of time (Dang et al., 2020).

Jamialahmadi et al.(2006) determined the oil-gas diffusivity by monitoring the oil swelling inside a high-pressure high-temperature cell. Using this technique, it is possible to maintain constant pressure and the tests could also be performed at high temperatures.

Recent studies have also shown the importance of oil swelling in the diffusion mechanism. Among the various recovery mechanisms proposed responsible for mass transport in unconventional

reservoirs, the following four mechanisms are the most cited and presented to be the most significant (Hoffman and Reichhardt ,2019):

- Pressure support
- Oil swelling
- Vaporization
- Viscosity reduction

Although these mechanisms are inter-related, Hoffman and Reichhardt (2020) present the relative contribution of each to the recovery, highlighting the importance of oil swelling mechanism. The simulation study is done for different cases of fracture surface area, injection time and reservoir permeability. The results conclude that although the contribution of vaporization increases with: (i) decreasing the fracture surface area, (ii) increasing injection time and (iii) higher matrix permeability, the dominant mechanism responsible for recovery is still oil swelling (**Figure 7**).

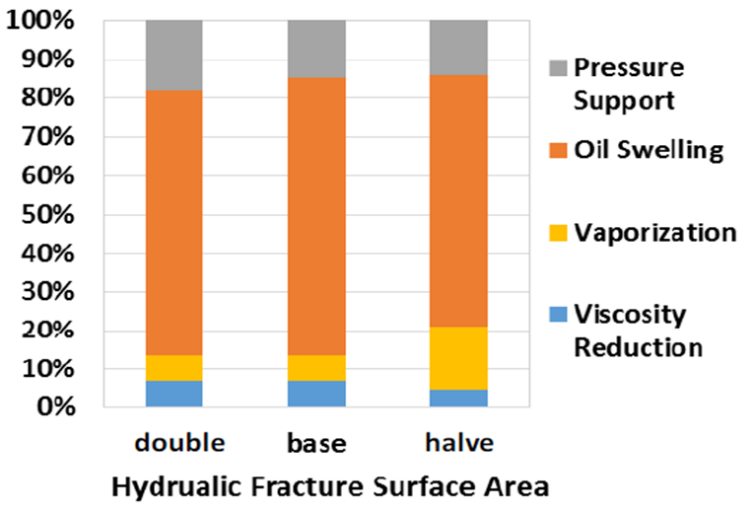

(a)

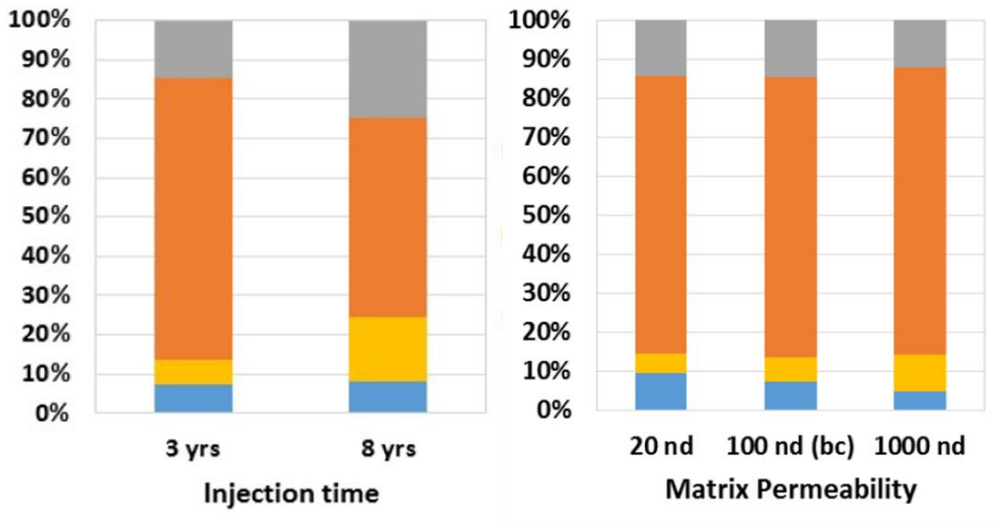

(b) **(c)**

Figure 7. Contribution of different mechanisms in recovery using models with (a) three different values of fracture surface area (b) different duration of injection time (c) different values of matrix permeability. Although, the respective contribution of vaporization increases with decreasing the fracture surface area, increasing the duration of injection gas and due to higher matrix permeability, oil swelling is still the dominant mechanism responsible for recovery (Hoffman and Reichhardt, 2020).

In this study, we have utilized a similar technique as Jamialahmadi et al., (2006), and have used the oil swelling data to derive the diffusion coefficient based on Fick's second law. This study focusses on the following points:

i. Measurement of diffusion coefficients of gas in oil using oil swelling technique. Three different oils (Eagle Ford, Meramec and Wolfcamp A) and three gas compositions (pure methane, and two methane/ethane mixtures (95/5 mole% and 72/28 mole%)) are used in this study.

ii. Investigation of the parameters which affect the measured diffusion coefficient. We have evaluated the impact of injection pressure, injected gas composition and liquid properties (API gravity and viscosity) on oil-gas diffusion coefficient at 175°F. A wide

range of pressures are studied, especially above and below the MMP of oil and gas mixtures under study.

iii. The effect of diffusion coefficient on the gas penetration depth and amount of gas injected is studied, considering an assumed tortuosity in the porous media.

1.1 Organization of Chapters

The thesis is divided into four chapters and is organized as follows:

- Chapter 2 is a brief review of equipment used, sample description, and experimental methodologies for measurement of MMP and oil gas diffusion coefficients.
- Chapter 3 describes the major findings of this study and discusses their field implications.
- Chapter 4 presents the conclusion and the most significant findings.

Chapter 2: Methodology

For this study, MMP of oil gas mixtures and their diffusion coefficients were measured at 175°F, over a wide range of pressures and with different combination of injection gases.

2.1 Sample description

Three injection gas compositions, including pure methane, methane /ethane mixtures (95/5 mole% and 72/28 mole%) and three oils (description shown in the Table 2), were used in this study. The measurement of API gravity and viscosity is done according to standards ASTM D-1250 and ASTM D-446, respectively. The compositions of the oil samples are detailed in Appendix A.

Oil	API gravity	Viscosity, cP
Wolfcamp A (WCA)	**32**	**6.1**
Meramec	**43**	**5.3**
Eagle Ford (EF)	**53**	**4.1**

Table 2. API gravity and viscosity of three oils used in this study. Amongst the three oils, Wolfcamp A oil is the heaviest and Eagle Ford oil is the lightest.

2.2 Experimental setup

Figure 8 shows a schematic of the apparatus used in the study. It consists of a high-pressure high-temperature cell which can be operated up to 10,000 psi internal pressure, 350^{o}F and has a cell volume of 50 cc. It is housed inside an oven to regulate temperature. The transparent glass windows allow the capture of the time-lapsed position of the oil-gas contact. Oil is injected into the cell from the lower cell inlet, and gas is injected at test pressures from the upper cell inlet (**Figure 8-b**).

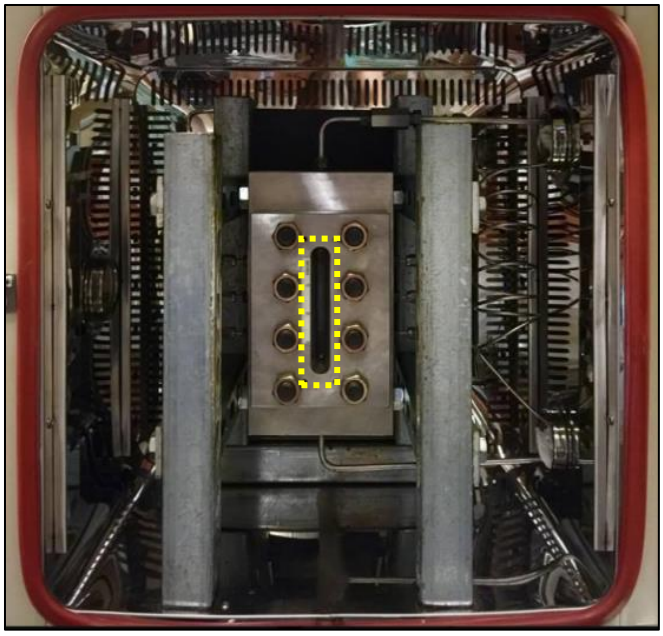

(a)

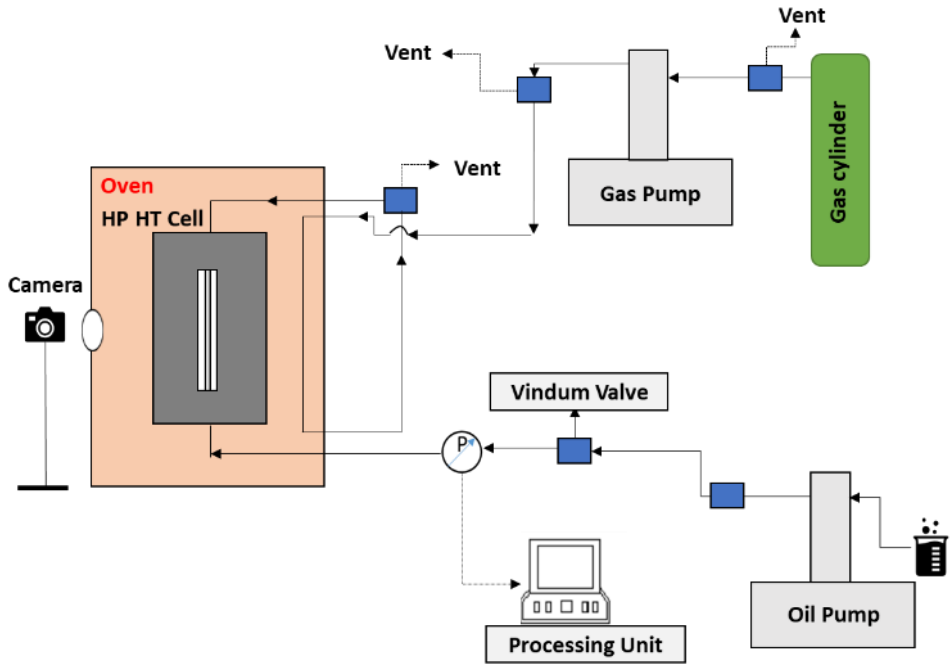

(b)

Figure 8. (a) High pressure-high temperature cell with a transparent window (yellow box). The cell is housed inside an oven to achieve a target temperature prior to tests. (b) The schematic shows the complete experimental apparatus. The cell has pressure and temperature capabilities of 10,000 psi and 350°F, respectively, and is connected to a gas pump (from the upper inlet) and an oil pump (from the lower inlet).

2.3 Minimum Miscibility Pressure – Vanishing Interfacial Tension (VIT) technique

The high pressure – high temperature cell is used to measure the MMP of an oil with a solvent gas. **Figure 9** shows a front view of the cell below MMP and above MMP. The capillary tube in the cell is placed to observe the rise of liquid in the tube. As the solvent gas is injected into the system, the height of the liquid meniscus in the capillary decreases. Once the injection pressure reaches the point of miscibility, the interface between oil and gas in the capillary tube vanishes. At every pressure step, an image of the VIT cell is taken. The capillary height is then measured from this image using ImageJ software and is plotted against the pressure steps to obtain the point of zero capillary height and thus zero interfacial tension, giving the MMP for the oil gas mixture, **Figure 10** shows the MMP value of Meramec oil and methane gas is equal to 5500 psi.

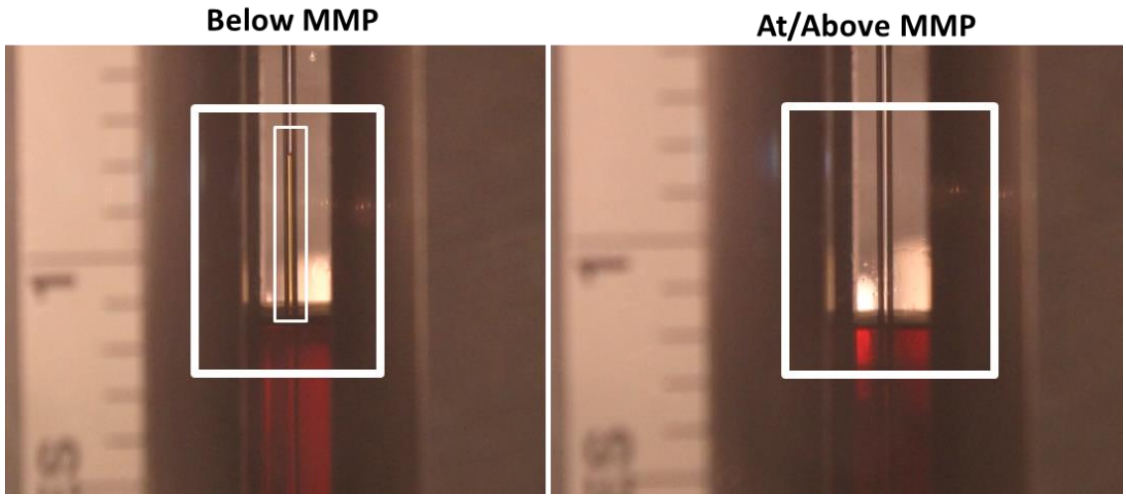

Figure 9. Zoomed image of the front view of high-pressure high-temperature cell with capillary tube (0.58 mm) inside it. The image on left indicates the presence of liquid in the capillary below MMP. At or above MMP, the oil gas interface in the capillary disappears.

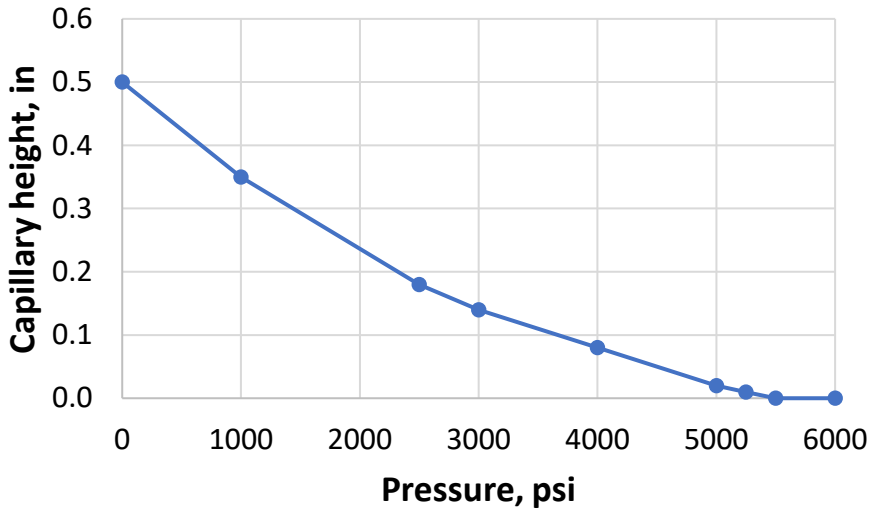

Figure 10. Capillary height versus pressure plot. For Meramec oil- pure methane gas mixture, the MMP is 5500 psi.

2.4 Oil swelling

The same high-pressure high-temperature cell is used for the oil swelling tests. Prior to each test, the cell is cleaned with acetone to remove any impurities. Oil is injected from the lower inlet and is filled to 60% of cell volume (30 cc). All the outlet valves are then closed, and the oven is set at the desired temperature (175^{o}F) for at least 12 hours. Gas is then injected into the cell at the desired pressure, which would be maintained constant throughout the experiment via the gas pumping system. The high definition camera acquires images at uniform logarithmic intervals of time and the change in the level of oil gas contact provides the oil swelling profile. The diffusion coefficient is determined using this oil swelling profile. The experiment spans a time interval of 6-8 days (**Figure. 11**).

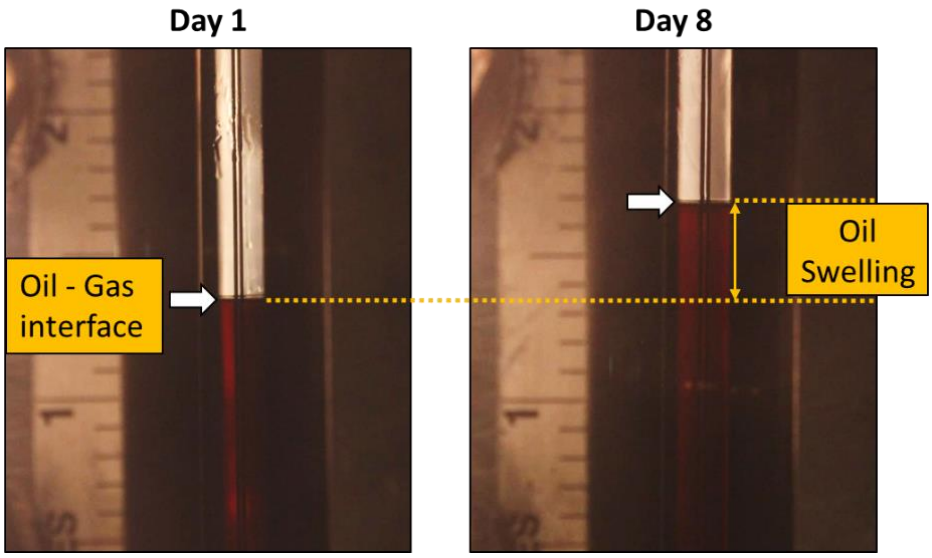

Figure 11. Measurement of oil swelling by monitoring the level of oil-gas contact in the cell over 8 days. Note: the capillary tube replicates the Minimum Miscibility Pressure (MMP) measurement using Vanishing Interfacial Tension (VIT) technique (Hawthorne et al., 2016); at above MMP there is no capillary rise in the tube.

2.5 Determination of bulk diffusion coefficient

With the acquired oil swelling profiles, the diffusion coefficient can be determined using the Fick's second law (Eq. 2). The diffusion of gas across the oil – gas interface changes the height of liquid column in the cell which can be translated to change in liquid volume in the cell. This rate of change of liquid phase volume can be described by the Eq., 3 (Jamialahmadi et al., 2006).

$$\frac{\partial C_a}{\partial t} = \mathrm{D}\,\frac{\partial^2 \mathrm{C_a}}{\partial \mathrm{x}^2} \tag{2}$$

$$\frac{dV}{V} = d(v_A \bar{C}_A) \tag{3}$$

Modifying Eqs. 2 and 3, we derive Eq. 4 which is used to estimate the final value of diffusion coefficient. For Eq. 4, we have used the rate restriction moving boundary condition (Whitman,

1923) which states that at a specific pressure-temperature condition, there can be a maximum concentration of gas that can dissolve into the oil phase. For this study, this maximum gas concentration in liquid phase (Ca) is estimated from the oil swelling profile as a function of time for different oil-gas mixtures and pressures.

$$\overline{C_a} exp(\vartheta_a \overline{C_a}) = \left(\frac{2C_{ai}}{Z_o}\sqrt{\frac{D}{\pi}}\right)\sqrt{t} \quad (4)$$

Nomenclature for equations 2, 3 and 4:

Ca	Concentration of solvent (kg/m^3)
t	Time (s)
D	Diffusion coefficient (m^2/s)
x	Distance from interface (m)
$\overline{C_a}$	Mean concentration of gas in oil phase (kg/m^3)
Cai	Interfacial concentration of solute (kg/m^3)
Zo	Initial position of interface (m)
ϑ_a	Molar volume of solute (m^3)

Chapter 3: Results and Discussions

3.1 Minimum Miscibility Pressure (VIT Technique)

First Contact MMP (FC-MMP) is measured using the Vanishing Interfacial Tension Technique (VIT). In this method, the observed interfacial tension is associated with the capillary rise in a small glass capillary tube (ID=0.58 mm). The pressure at which the capillary rise disappears, is considered as FC-MMP.

At a specific temperature condition, MMP is influenced by the injectate gas composition and the oil composition. Using the same injection gas – C1/C2(72/28), the oil sample with a higher concentration of intermediate and light fractions is observed to have a lower MMP. Amongst the three oils under study, EF oil being the lightest has the lowest MMP (3550 psi) and WCA oil being the heaviest, has the highest MMP (5700 psi) with C1/C2(72/28) gas. We also observe that with the enrichment of ethane in the injection gas, the MMP values decrease (**Figure. 12**).

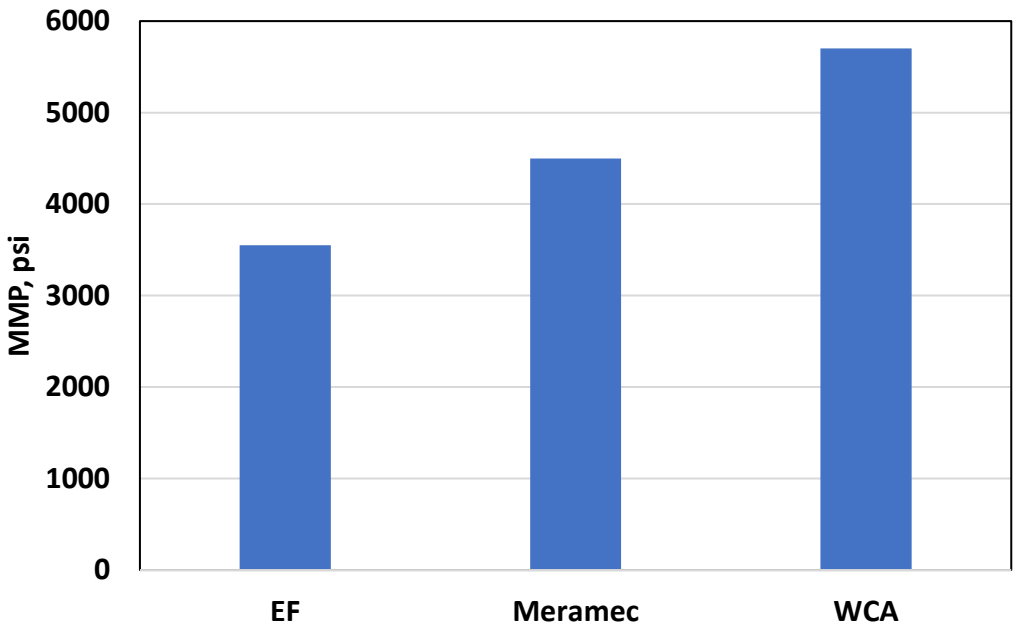

(a)

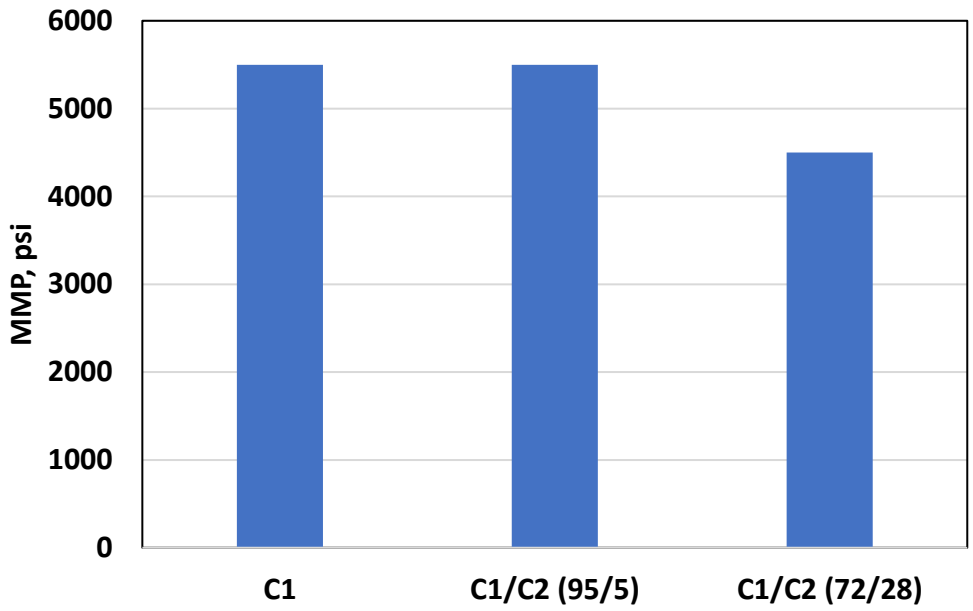

(b)

Figure 12. Summary of FC-MMP measures using the VIT technique for different oil samples with different injection gas compositions at the same temperature (175F). (a) With the same injection gas (C1/C2 (72/28)), the oil sample with higher API gravity is observed to have lower values of FC-MMP. (b) For Meramec oil sample, the injection gas with richer ethane concentration has a reduced FC-MMP.

3.2 Oil Swelling

The oil swelling profiles for the Meramec oil sample with C1/C2(72/28 mole%) gas at different pressures (3500 psi – 5500 psi) are shown in **Figure 13**. After 8 days, we observe that the final oil swelling percentage increases as a function of pressure. However, the initial rate of swelling is inversely proportional to the pressure, due to the increase of density and viscosity of the oil-gas system. With the acquired oil swelling profiles, the diffusion coefficient can be determined using the Fick's second law (Eq. 2).

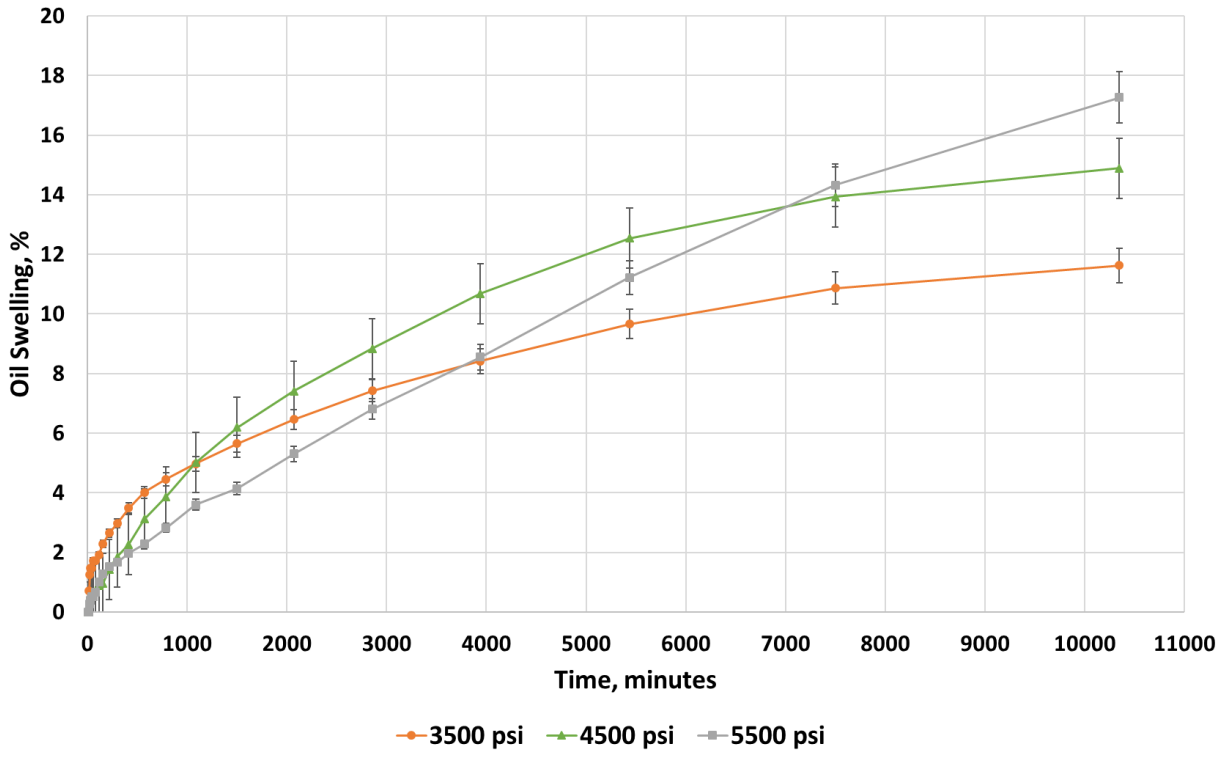

Figure 13. Oil swelling profiles for Meramec oil – C1/C2(72/28 mole%) system for 3 different pressures at 175°F. The total oil swelling increases as a function of increasing pressure. However, due to increased density of oil – gas mixtures, the early rate of oil swelling decreases with increasing pressure.

3.3 Impact of injection pressure on diffusion coefficient

Figure 14 shows the diffusion coefficients for the Eagle Ford oil, Meramec oil and Wolfcamp A oil with the injection gas C1/C2 (72/28 mole%) as a function of pressure at 175°F. The MMPs for Eagle Ford oil, Meramec oil and Wolfcamp A oil with the injection gas C1/C2 (72/28 mole%) are 3550 psi, 4500 psi, and 5700 psi, respectively. We observe that for all the oil-gas combinations, the diffusion coefficient first increases as the pressure is increased from below MMP to the point of MMP and then decreases beyond MMP. Jamialahmadi et al., (2006) also observed a decrease of diffusivity beyond MMP for pure methane gas and dodecane mixture (**Figure 15**). This behavior can be attributed to the increase in density and viscosity of the oil-gas solution. For a particular

oil-gas combination, the increase in diffusion coefficient below MMP can be attributed to the increase of miscibility. Above MMP, when complete miscibility is achieved, the increase in fluid density and viscosity lead to the decrease of diffusion coefficient (Appendix B).

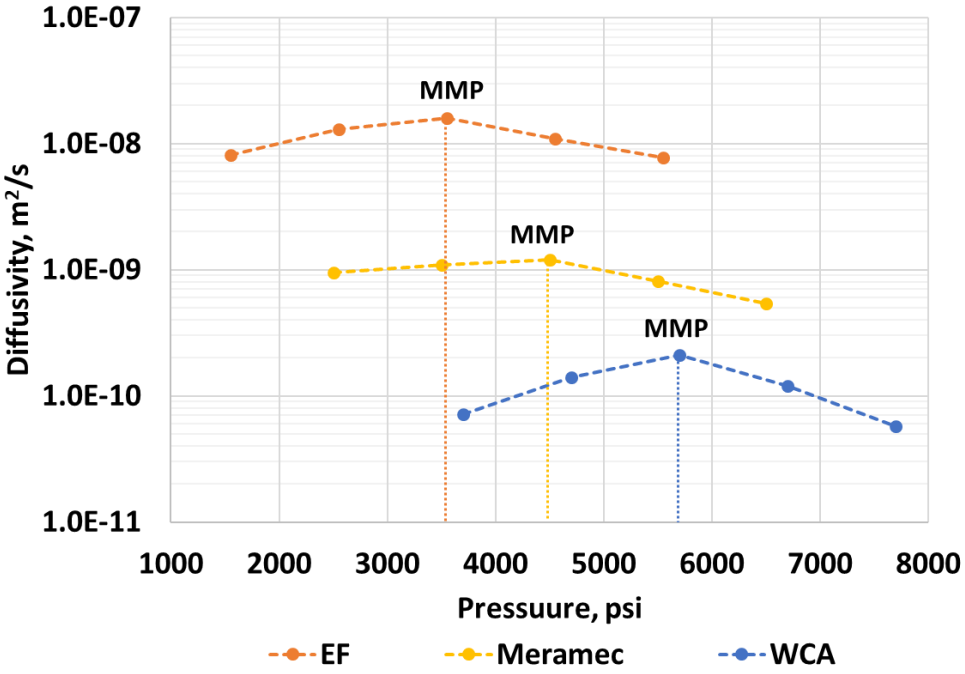

Figure 14. Diffusion coefficient of C1/C2(72/28 mole%) gas in Eagle Ford oil, Meramec oil and Wolfcamp A oil as a function of pressure at 175°F. Below MMP, diffusion coefficient increases with increasing pressure. Beyond MMP, due to increase in density and viscosity of the solution, diffusion coefficient decreases as a function of increasing pressure.

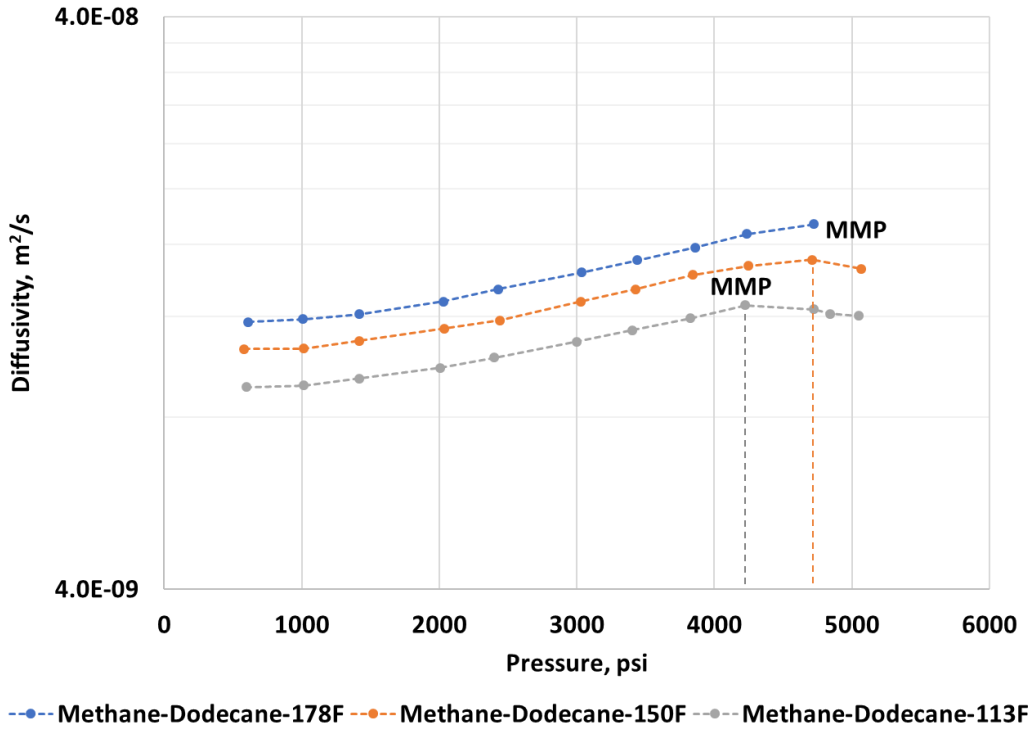

Figure 15. Diffusivity of methane gas in dodecane as a function of pressure and temperature. Beyond MMP, the diffusivity values decrease due to the increase in density and viscosity of the solution. (Modified after Jamialahmadi et al., 2006)

3.4 Impact of injection gas composition on diffusion coefficient

The measured diffusion coefficients for the Meramec oil sample and three different gas injectates at the same pressure temperature conditions are shown in **Figure 16**. The diffusion coefficient increases with the increase in ethane composition in the gas up to three-fold; from 2.9E-10 m^2/s with pure methane to 9.5E-10 m^2/s with C1/C2(72/28 mole%) Amongst the three gas mixtures used, C1/C2 (72/28 mole%) mixture results in the highest diffusion of gas in oil. Thus, gas enrichment can benefit the huff-n-puff process by increasing the diffusivity and shortening the soaking time.

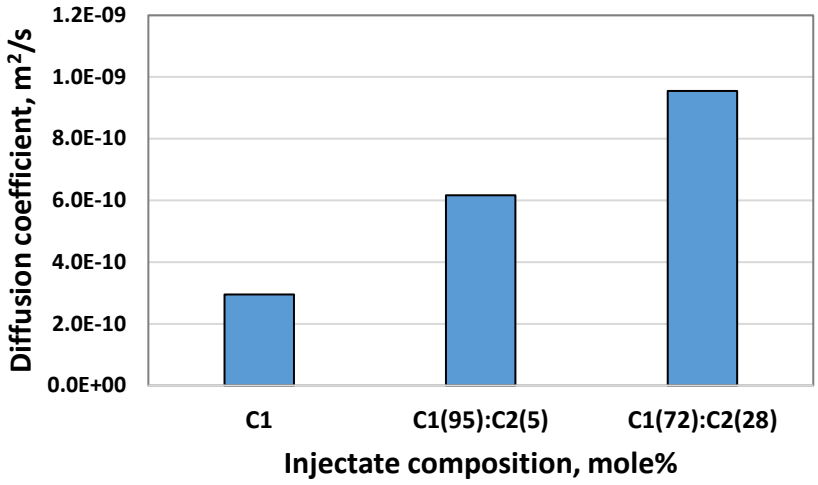

Figure 16. Diffusion coefficient of gas in oil as a function of injectate composition at constant pressure of 2500 psi and 175°F. Enrichment in injectate gas composition results in an increase of the oil – gas system diffusion coefficient.

3.5 Impact of API gravity and viscosity of oil on diffusion coefficient

Figure 17 shows the diffusion coefficients for the Wolfcamp A oil, Meramec oil and Eagle Ford oil with the injection gas C1/C2 (72/28 mole%) at their respective MMPs at 175°F. The MMPs for Eagle Ford oil, Meramec oil and Wolfcamp A oil with the injection gas C1/C2 (72/28 mole%) are 3550 psi, 4500 psi, and 5700 psi, respectively. We observe that for the oil-gas combinations, the diffusion coefficient increases as the API gravity increases and viscosity decreases. Higher API gravity and lower viscosity corresponds to an oil with more light and intermediate components as compared to oil with lower API gravity and higher viscosity. For the comparison, Eagle Ford oil has the highest diffusion coefficient and Wolfcamp A oil has the lowest; the difference is as much as two orders of magnitude. It is important to mention that the previous mentioned parameters (injection pressure and injected gas composition) can be controlled by operating parameters but the fluid properties (API gravity and viscosity) cannot be constrained. However, knowing these properties can help in deciding the operating parameters while designing EOR strategies.

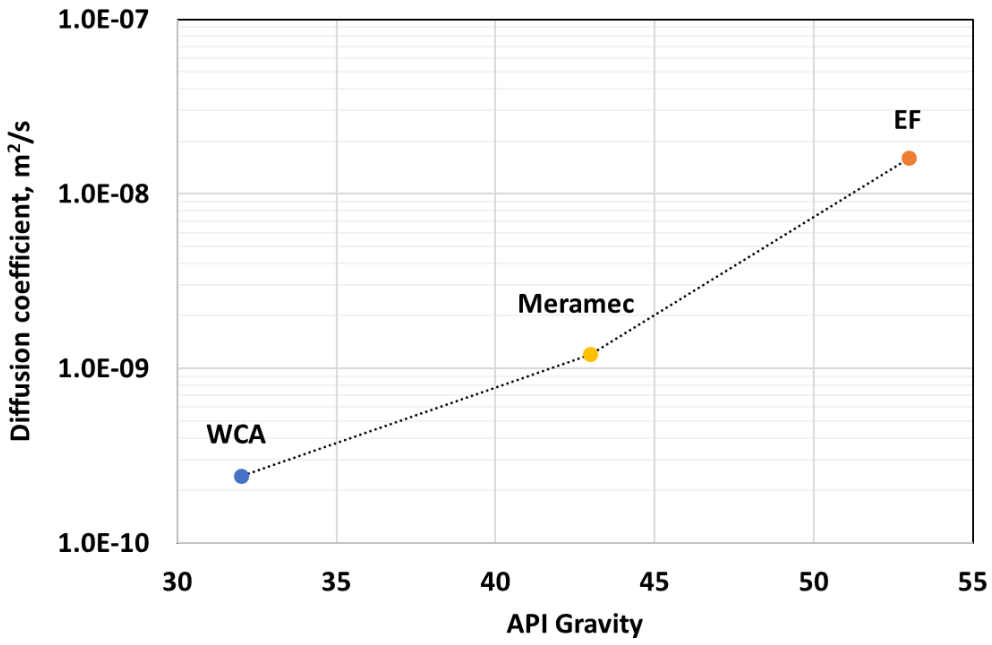

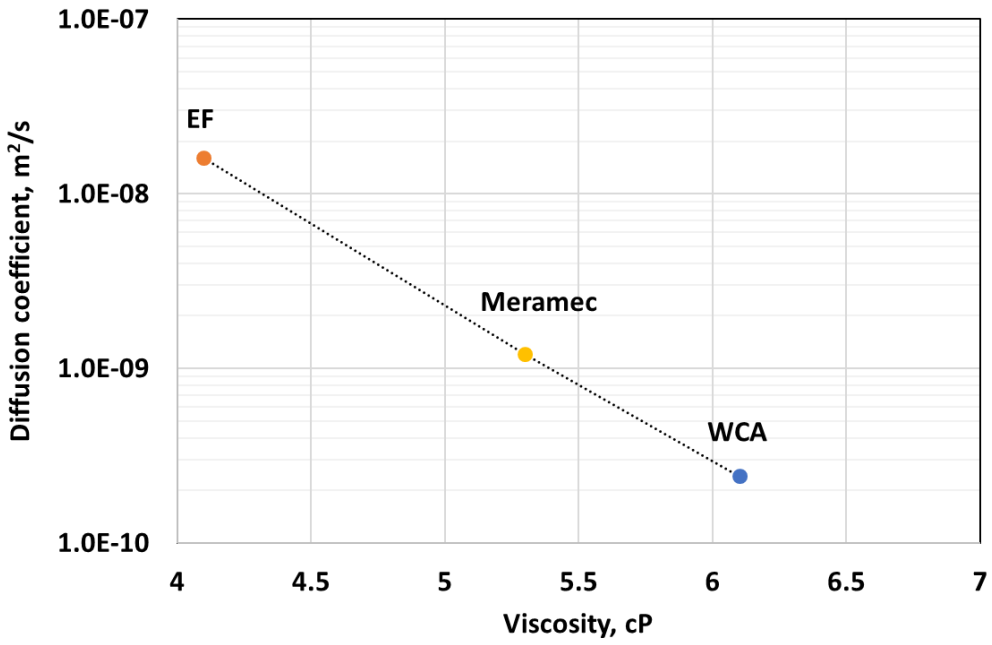

Figure 17. Diffusion coefficient of C1/C2(72/28 mole%) gas in WCA oil, Meramec oil and EF oil at their respective MMPs (5700 psi, 4500 psi and 3550 psi) and 175°F as a function of API gravity and viscosity of oils. As the API gravity of oils increase and the viscosity decreases, the diffusion coefficients at the point of their respective MMPs increase.

3.6 Gas concentration profiles

Gas travel into the matrix can be modeled using the Fick's second law (Eq. 2). It can be solved for the following boundary conditions (Hoffman and Rutledge, 2019):

- t=0, gas concentration in fracture =1
- t=0, gas concentration in matrix = 0
- t>0, gas concentration in fracture = 1

Applying the boundary conditions to the Eq. 2, we obtain the concentration profile of the gas travelling into the matrix (Crank, 1975) as:

$$C(x,t) = erfc\left(\frac{x}{\sqrt{4Dt}}\right) \quad (5)$$

Matrix tortuosity impacts the diffusion efficiency in porous media and this value can vary over a wide range (Chen et al., 1977; Flurry and Brosse, 2017; Dang et al., 2018). Unlike conventional rocks with a narrow range of tortuosity, e.g.1-4, tight rocks can have a wide range of tortuosity, i.e. 4-16. Tortuosity directly impacts the effective diffusivity and can provide information about how effectively miscible gases can penetrate into the rock matrix. Calculating the gas penetration depth for the most optimum and least optimum cases for diffusivities for Meramec oil and 72/28 mixtures, we see that the depth of penetration is still less than a foot (**Figure 18**). One more thing to note is the tortuosity assumed in this calculation is the optimum value of 5, which is rare to find in field conditions. Keeping all conditions the same but considering the worst case of tortuosity , i.e.15, we see that the maximum depth the gas diffuses in 6 months is 0.5 ft (**Figure 19**). Thus, we observe that, as tortuosity increases three-fold for constant diffusivity values, the maximum distance that the injectate travels reduces significantly which can impact the sweep efficiency and the production from the reservoir.

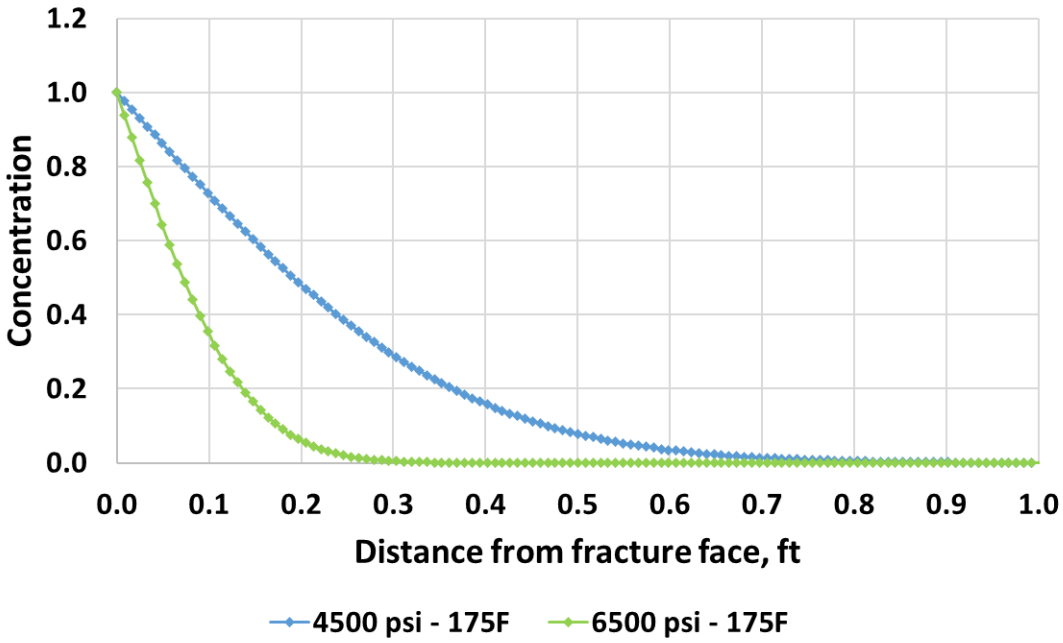

Figure 18. Gas penetration depth for C1/C2 (72/28) gas – Meramec oil system at 175°F at two different pressures. The maximum distance the gas travels away from the fracture face for a tortuosity value of 5 is 0.9 ft. The diffusivity values at 4500 psi and 6500 psi are 1.2 x 10^{-9} m^2/s and 5.3 x 10^{-10} m^2/s.

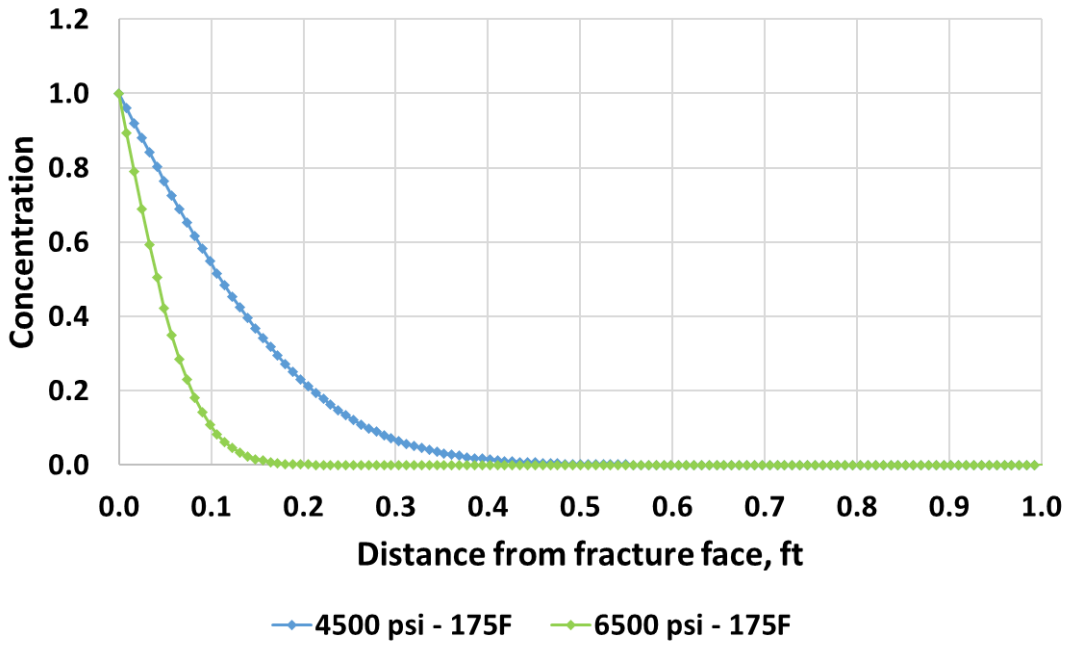

Figure 19. Gas penetration depth for C1/C2 (72/28) gas – Meramec oil system at 175°F at two different pressures. The maximum distance the gas travels away from the fracture face for a tortuosity value of 15 is 0.5 ft. The diffusivity values at 4500 psi and 6500 psi are 1.2 x 10^{-9} m^2/s and 5.3 x 10^{-10} m^2/s.

On the field scale, these results may suggest the role of diffusion to be insignificant as a mass transport mechanism, however in the context of large stimulated reservoir surface – SRA (instead of stimulated reservoir volume – SRV), proposed and observed in field scale experiments (Raterman et al., 2017), the impact of diffusion can dominate. A fracture spacing of 2 – 4 ft (equivalent to the average of 15 – 25 fracture count per 50 ft) on core samples from horizontal observation wells parallel to a stimulated well has been observed (Raterman et al., 2017, **Figure 20**). This makes the ultimate diffusion length equal to 1 – 2 ft (half length of the fracture spacing). From the results, considering C1/C2(72/28) as injectate gas in Meramec oil for a tortuosity of 15 (**Figure 19**), the sweep efficiency can be increased from 20% to 50% when the diffusion coefficient doubles. Therefore, adjusting field parameters such as injection pressure, injection

time, injection gas composition can help to optimize diffusion coefficient and can lead to better EOR results.

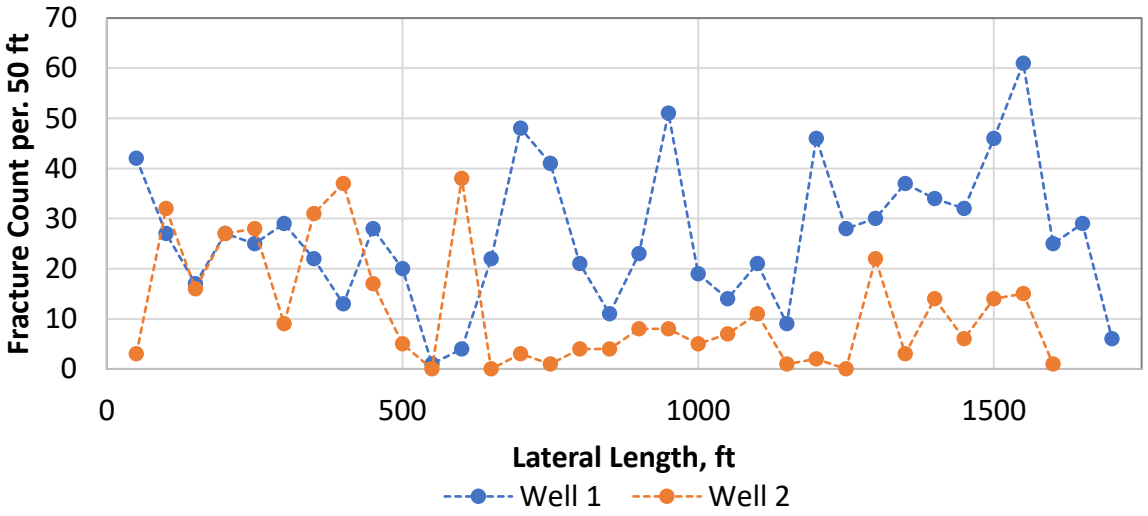

Figure 20. Fracture count per 50 ft of lateral wellbore in Eagle Ford cores. Well 1 is drilled horizontally near to stimulated well and shows average fracture spacing of 2 ft., while well 2 drilled vertically near to stimulated well shows average fracture spacing of 4 ft. The fracture density of the stimulated surface area is a function of the distance away from the stimulated well. (Raterman et al., 2017)

Figure 21 shows the gas penetration depth of C1/C2(72/28) gas in Meramec oil at 4500 psi (MMP) for 1 month, 3 months and 6 months. From the results, it is apparent that the gas travels deeper into the rock matrix with increasing soak periods and the depth of penetration is a function of square root of time (Eq. 5). For field EOR operations, knowing the depth of penetration during a huff phase can help regulate the compressor rotation scheme between the wells and thus optimize their cost.

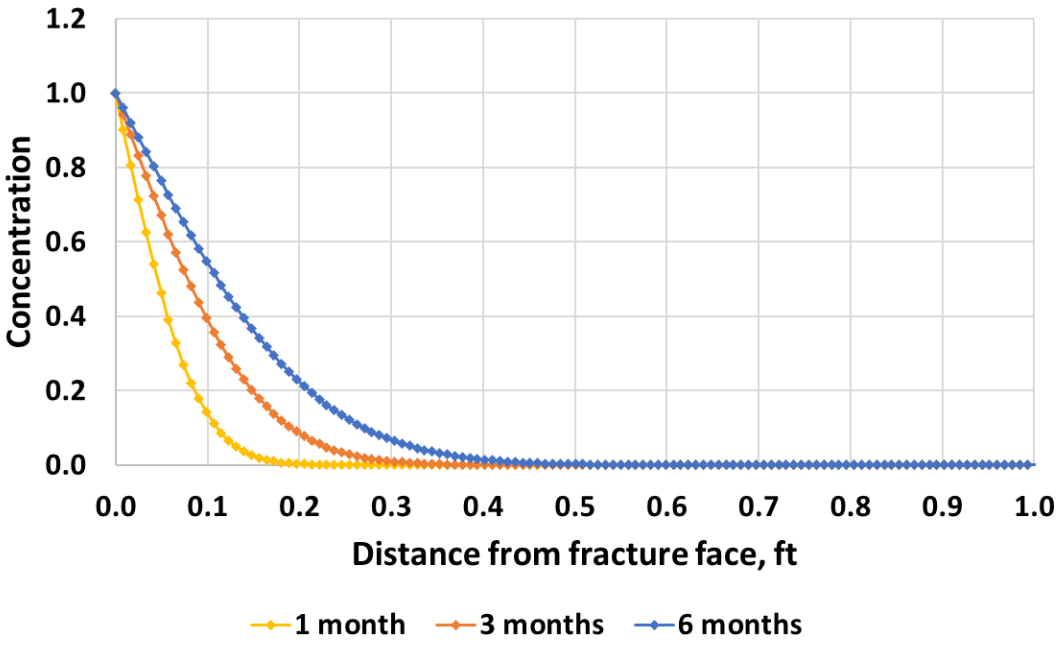

Figure 21. Gas penetration depth for C1/C2 (72/28) gas – Meramec oil system at 4500 psi and 175°F for 3 soaking periods (1 month, 3 months and 6 months). The maximum distance the gas travels away from the fracture face for a tortuosity value of 15 is 0.5 ft. The oil-gas diffusivity at 4500 psi is 1.2 x 10^{-9} m^2/s.

Figure 22 shows the gas penetration depths for the WCA oil, Meramec oil and Eagle Ford oil with C1/C2(72/28) gas at their respective MMPs, 5700 psi, 4500 psi and 3550 psi, for 6 months of injection. A constant tortuosity value of 15 has been used for the calculations to emphasize the impact of diffusion on the gas penetration depth in the different oil-gas combinations. It is evident from the results that increasing the diffusivity by two orders of magnitude (from WCA oil- 2.4 x 10^{-10} m^2/s to EF oil- 1.6 x 10^{-8} m^2/s), the depth of penetration increases from 0.2 ft for WCA oil to 1.4 ft for EF oil.

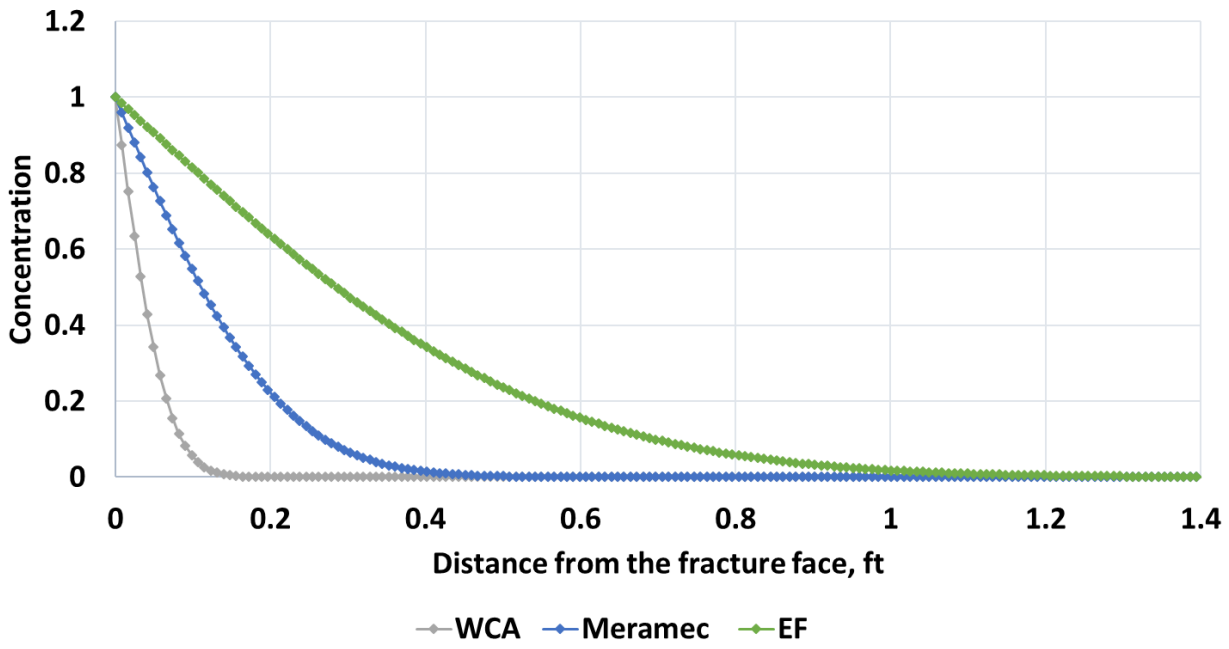

Figure 22. Gas penetration depth for C1/C2 (72/28) gas with WCA oil, Meramec oil and EF oil at their respective MMPs, 5700 psi, 4500 psi and 3550 psi and 175°F for 6 months. For a constant tortuosity of 15 for all the formations, the gas penetration depth increases with increase in diffusion coefficients. The oil-gas diffusivity for WCA oil, Meramec oil and EF oil at their MMPs is 2.4 x 10^{-10} m^2/s, 1.2 x 10^{-9} m^2/s and 1.6 x 10^{-8} m^2/s respectively.

We can also calculate the amount of gas diffused into the matrix by integrating the concentration curves. Assuming a porosity of 6% and gas formation volume factor of 0.01 res. ft^3/scf, the total reservoir volume of gas is 5 scf per unit fracture surface area. For an assumed fracture surface area of 10 million ft^2, the volume of gas penetrating into the matrix due to diffusion, for the blue curve in **Figure 19** (4500 psi for 6 months) will be 50 million scf. If we reduce the diffusion coefficient to half by modifying the injection pressure to 6500 psi (**Figure 19**, green curve); the amount of gas injected into the matrix due to diffusion would change from 50 million to only 5 million scf, other assumptions remaining same.

These calculations are useful in deciding EOR designs to:

- find how much gas goes into the formation,
- the penetration distance of the injected gas,
- optimizing compressor cost, compressor rotation schedule for different wells and cost of injected gas.

Chapter 4: Conclusions

Huff-n-Puff cyclic injection has shown promising results for the enhanced oil recovery in the unconventional reservoirs(Thomas and Monger, 2007). While pilot tests resulted in increased recovery using this method, the underlying mechanism for the additional recovery is still not well understood. Recent studies suggest the dominance of diffusion mechanism in Huff-n-Puff EOR in tight rocks. This study proposes a technique to measure oil-gas diffusion coefficients from oil swelling and evaluates the parameters governing diffusion. We investigate the impact of injection pressure, injectate composition, API gravity and viscosity of oil on the diffusivity of oil gas mixtures.

The following conclusions can be drawn from the results of our study:

1. For all the oil-gas combinations, the diffusion coefficient first increases as the pressure is increased from below MMP to the point of MMP and then decreases beyond MMP. This behavior can be attributed to the increase in density and viscosity of the oil-gas solution with pressure

2. Enrichment of injection gas can increase the oil-gas diffusion coefficient and can aid in reducing the soaking time.

3. The diffusion coefficient increases as the API gravity of oil increases and viscosity of oil decreases. Higher API gravity corresponds to an oil with more light and intermediate components as compared to lower API gravity oil. Although this parameter cannot be constrained, knowing the oil properties can help regulate other operating parameters like injection pressure and injection gas composition.

4. Regardless of injection pressure, for the gas mixture C1/C2 (72/28 mole%) the diffusion coefficient varies between 10^{-11} m^2/s to 10^{-10} m^2/s for Wolfcamp A oil; 10^{-10} m^2/s to 10^{-9} m^2/s for Meramec oil and 10^{-9} m^2/s to 10^{-8} m^2/s for Eagle Ford oil.

5. Matrix tortuosity impacts the diffusion efficiency in porous media. Based on the diffusion coefficients determined in this study for Meramec oil- C1/C2(72/28 mole%) gas, the sweep efficiency can be increased from 20% to 50% by increasing the bulk diffusion coefficient from 5.3×10^{-10} m^2/s to 1.2×10^{-9} m^2/s.

6. A knowledge of amount of gas required to inject and its penetration depth into the formation can help in optimizing the compressor schedule in field and the economics of the EOR design.

The study emphasizes that having the richer injectate composition at the right pressure can help in optimizing the huff-n-puff recovery in shales. The data reported in this study can help improve existing EOR parameters and can be used for designing EOR strategies for new areas.

It is also important to highlight that although oil swelling mechanism has significant contribution to the oil-gas diffusion phenomenon; it is not the only mechanism responsible for additional recovery. Recent research has shown that during diffusion, vaporization also contributes to the recovery and it is recommended to be explored as future work.

References

1. Amman-Hildebrand, A., Ghanizadeh, A. and Kross, B. M., 2012. Transport properties of unconventional gas systems. Marine and Petroleum Geology 31: 90-99 https://doi.org/10.1016/j.marpetgeo.2011.11.009
2. Chen, L.L.Y., Katz, D.L. and Tek, M. R., 1977. Binary gas diffusion of methane-nitrogen through porous media. AIChE Journal, Vol. 23, No. 3, 336. https://doi.org/10.1002/aic.690230317
3. Crank, M., 1975. The mathematics of diffusion: Second edition, Oxford University Press, London. 414p.
4. Cronin, M., Emami, H. and Johns, R. T., 2018. Diffusion-dominated proxy model for solvent injection in ultra-tight oil reservoirs. Society of Petroleum Engineers. doi:10.2118/190305-MS
5. Dang, S. T., Sondergeld, C. H., Rai, C. S., Tinni, A, O. and Drenzek, N., 2018. A first step in evaluating the role of diffusion in EOR in tight shale formations. SCA-2018
6. Dang, S. T., Sondergeld, C. H. and Rai, C. S., 2020. Novel technique to measure mutual bulk fluid diffusion using NMR 1-D gradient. E3S Web Conf. 146 03007. doi: 10.1051/e3sconf/202014603007
7. Dang, S., 2019. Understanding the fundamental drive mechanisms for Huff-n-Puff EOR in tight formations. Ph.D. Thesis, University of Oklahoma.
8. Denoyelle, L. and Bardon, C., 1983. Influence of diffusion on enhanced oil recovery by CO2 injection. Proceedings International Symposium on CO2 Enhanced Oil Recovery, Budapest, Hungary.

9. Energy Information Administration (EIA), 2019. U.S. Field Production of crude oil, https://www.eia.gov/dnav/pet/hist/LeafHandler.ashx?n=PET&s=MCRFPUS1&f=M
10. Fleury, M. and Brosse, E., 2017. Transport in tight rocks. AGU Hydrobiogeochemical Properties of Caprock, June 2017.
11. Gamadi, T. D., Sheng, J. J., Soliman, M. Y., Menouar, H., Watson, M. C. and Emadibaladehi, H., 2014. An experimental study of cyclic CO2 injection to improve shale oil recovery.
12. Guo, P., Wang, Z., Shen, P. and Du, J., 2009. General research: Molecular diffusion coefficients of the multicomponent gas-crude oil systems under high temperature and pressure. Industrial and Engineering Chemistry Research, 48(19), 9023–9027. https://doi.org/10.1021/ie801671u
13. Hawthorne, S. B., Gorecki, C. D., Sorensen, J. A., Steadman, E. N., Harju, J. A. and Melzer, S., 2013. Hydrocarbon mobilization mechanisms from upper, middle, and lower Bakken reservoir rocks exposed to CO2. Society of Petroleum Engineers. doi:10.2118/167200-MS
14. Hawthorne, S. B., Miller, D., Jin, L., and Gorecki, C. D., 2016. Rapid and simple capillary-rise/Vanishing Interfacial Tension method to determine crude oil Minimum Miscibility Pressure: Pure and mixed CO2, methane, and ethane. Energy & Fuels. 30(8), 6365-6372. doi:10.1021/acs.energyfuels.6b01151
15. Hoffman, B. T. and Reichhardt, D., 2020. Sensitivity analysis of cyclic gas injection recovery mechanisms in unconventional reservoirs. Unconventional Resources Technology Conference. doi:10.15530/urtec-2020-2933

16. Hoffman, B. T., and Reichhardt, D., 2019. Quantitative evaluation of recovery mechanisms for Huff-n-Puff gas injection in unconventional reservoirs. Unconventional Resources Technology Conference. doi:10.15530/urtec-2019-147
17. Hoffman, T. B. and Evans, J. G. 2016. Improved Oil Recovery (IOR) pilot projects in the Bakken formation. Society of Petroleum Engineers. doi:10.2118/180270-MS
18. Hoffman, B. T. ,2018. Huff-N-Puff gas injection pilot projects in the Eagle Ford. Society of Petroleum Engineers. doi:10.2118/189816-MS
19. Hoffman, B. T. and Rutledge, J. M., 2019. Mechanisms for Huff-n-Puff cyclic gas injection into unconventional reservoirs. Society of Petroleum Engineers. doi:10.2118/195223-MS
20. Hoteit, H. and Firoozabadi, A., 2009. Numerical modeling of diffusion in fractured media for gas-injection and -recycling schemes. Society of Petroleum Engineers. doi:10.2118/103292-PA
21. Jamialahmadi, M., Emadi, M. and Müller-Steinhagen, H., 2006. Diffusion coefficients of methane in liquid hydrocarbons at high pressure and temperature. Journal of Petroleum Science and Engineering, 53(1–2), 47–60. https://doi.org/10.1016/j.petrol.2006.01.011
22. Li, L., Su, Y., Sheng, J. J., Hao, Y., Wang, W., L, Y. and Wang, H.,2019. Experimental and numerical study on CO2 sweep volume during CO2 Huff-n-Puff enhanced oil recovery process in shale oil reservoirs [Research-article]. Energy and Fuels, 33(5), 4017–4032. https://doi.org/10.1021/acs.energyfuels.9b00164
23. Li, L., Sheng, J. J. and Sheng, J., 2016. Optimization of Huff-n-Puff gas injection to enhance oil recovery in shale reservoirs. Society of Petroleum Engineers. doi:10.2118/180219-MS

24. Mobilia, M., Lieskovsky, J. and Yan, R., 2016. Initial production rates in tight oil formations continue to rise. U. S. Energy Information Administration, February 11, 2016. https://www.eia.gov/todayinenergy/detail.php?id=24932
25. Nagarajan, N. R., Stoll, D., Litvak, M. L., Prasad, R. S., and Shaarawi, K., 2020. Successful field test of enhancing Bakken oil recovery by propane injection: Part I. Field test planning, operations, surveillance, and results. Unconventional Resources Technology Conference. doi:10.15530/urtec-2020-2768
26. Nour, A. H., Yaacob, Z. Bin, and Alagorni, A. H., 2015. An overview of oil production stages: enhanced oil recovery techniques and nitrogen injection. International Journal of Environmental Science and Development, 6(9), 693–701. https://doi.org/10.7763/ijesd.2015.v6.682
27. Perkins, T. K., Johnston, O. C. and Hoffman, R. N.,1965. Mechanics of viscous fingering in miscible systems. Society of Petroleum Engineers Journal, 5(04), 301–317. https://doi.org/10.2118/1229-pa
28. Raterman, K. T., Farrell, H. E., Mora, O. S., Janssen, A. L., Gomez, G. A., Busetti, S. and Warren, M., 2017. Sampling a stimulated rock volume: An Eagle Ford example. SPE/AAPG/SEG Unconventional Resources Technology Conference 2017, 1–18. https://doi.org/10.15530/urtec-20172670034
29. Riazi, M.R. and Whitson, C.H., 1993. Estimation of diffusion coefficients of dense fluids. Ind. Eng. Chem. Res. 32, 3081–3088.
30. Riazi, M. R.,1996. A new method for experimental measurement of diffusion coefficients in reservoir fluids. Journal of Petroleum Science and Engineering, 14(3–4), 235–250. https://doi.org/10.1016/0920-4105(95)00035-6

31. Russel, J. and Dindoruk, B.,2013. Enhanced oil recovery field case studies: Chapter 1. Gas flooding. Elsevier Inc. Chapters.
32. Sigmund, P. M., 1976. Prediction of molecular diffusion at reservoir conditions, Part 1-measurement and prediction of binary dense gas diffusion coefficients, J. Can. Pet. Technol., 15, pp. 48-57.
33. Thomas, G. and Monger, T.,2007. Feasibility of cyclic CO2 injection for light-oil recovery. SPE Reservoir Engineering, 6(02), 179–184. https://doi.org/10.2118/20208-PA
34. Tovar, F. D., Barrufet, M. A. and Schechter, D. S., 2018. Gas injection for EOR in organic rich shale. Part I: Operational philosophy. Society of Petroleum Engineers. doi:10.2118/190323-MS
35. Wang, D., Butler, R., Liu, H. and Ahmed, S., 2010. Flow rate behavior in shale rock. Society of Petroleum Engineers. doi:10.2118/138521-MS
36. Wang, C., and Li, S.,(2019). The effect of fractures on gas injection in Hailar oilfield. Journal of Petroleum Exploration and Production Technology, 9(1), 409–416. https://doi.org/10.1007/s13202-018-0475
37. Wang, L., Tian, Y., Yu, X., Wang, C., Yao, B., Wang, S., Winterfeld, P. H., Wang, X., Yang, Z., Wang, Y., Cui J. and Wu, Y. S., 2017. Advances in improved/enhanced oil recovery technologies for tight and shale reservoirs. Fuel 210, 425-445
38. Whitman, W. G., 1923. The two-film theory of absorption. Chem. Metall. Eng., 29, pp. 147-152
39. Yu, W.; Lashgari, H. and Sepehrnoori, K., 2014. Simulation study of CO2 Huff-n-Puff process in Bakken tight oil reservoirs; Society of Petroleum Engineers: doi: 10.2118/169575-MS.

40. Zhang, Y., Hyndman, C., and Maini, B., (2000). Measurement of gas diffusivity in heavy oils. Journal of Petroleum Science and Engineering, 25(1–2), 37–47. https://doi.org/10.1016/S0920-4105(99)00031-5

Appendix A

Figure 23, 24 and 25 show the detailed composition analysis on the oil samples used for this study (Personal Communication: Stratum Reservoir Labs, Houston).

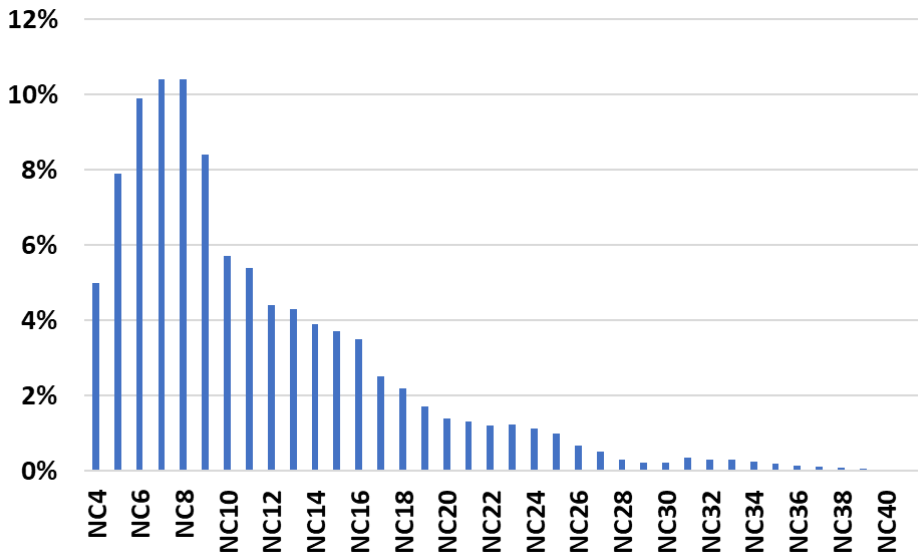

Figure 23. Detailed compositional analysis on Eagle Ford oil (API gravity – 53 and Viscosity – 4.1 cP)

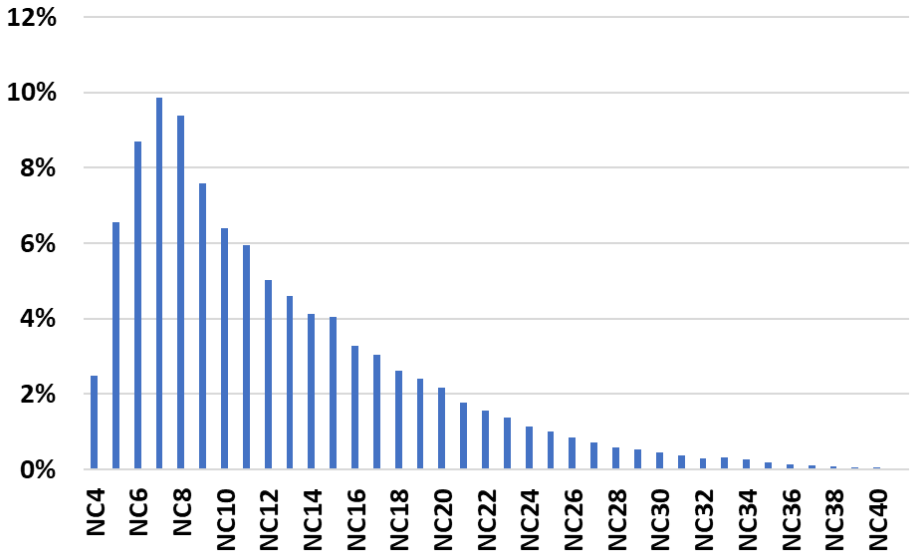

Figure 24. Detailed compositional analysis on Meramec oil (API gravity – 43 and Viscosity – 5.3 cP)

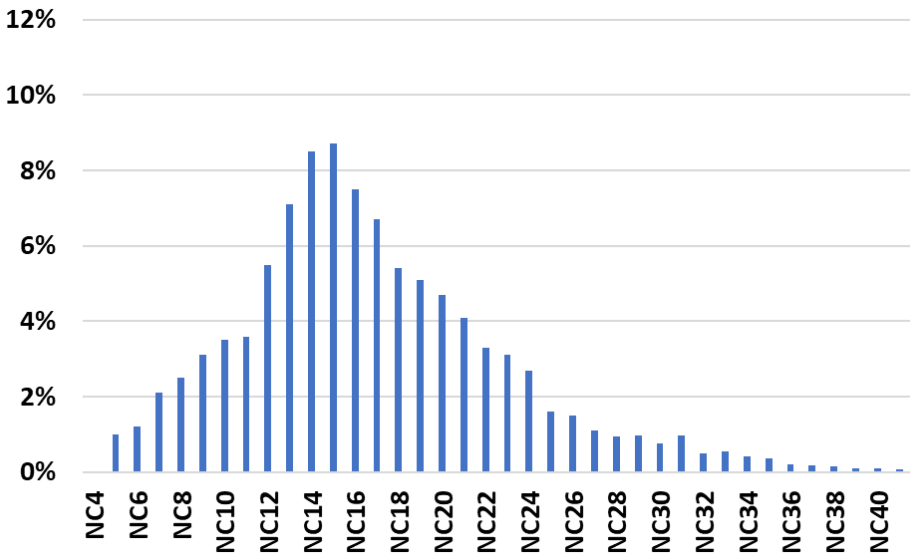

Figure 25. Detailed compositional analysis on Wolfcamp A oil (API gravity – 32 and Viscosity – 6.1 cP)

Appendix B

Figure 26 and 27 show the increase in fluid density and viscosity of the solution (Meramec oil - C1/C2(72/28) gas) as a function of temperature and pressure. The reduction in diffusion coefficient beyond the point of MMP (**Figure 14**) can be attributed to the increase in density and viscosity of the solution. For a particular oil-gas combination, the increase in diffusion coefficient below MMP can be attributed to the increase of miscibility. Above MMP, when complete miscibility is achieved, the increase in fluid density and viscosity lead to the decrease of diffusion coefficient.

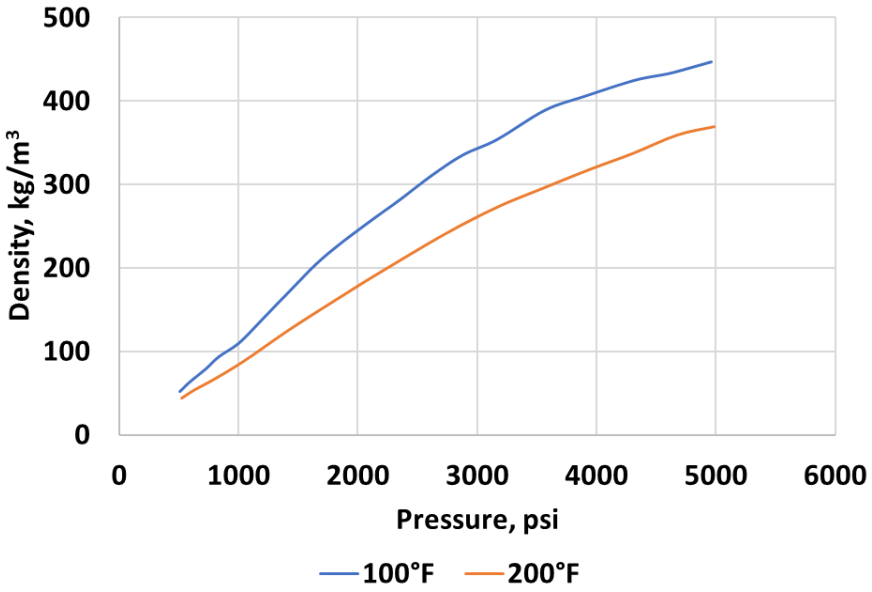

Figure 26. Variation of solution (Meramec oil-C1/C2(72/28) gas) density as a function of pressure and temperature (from PVTSim software)

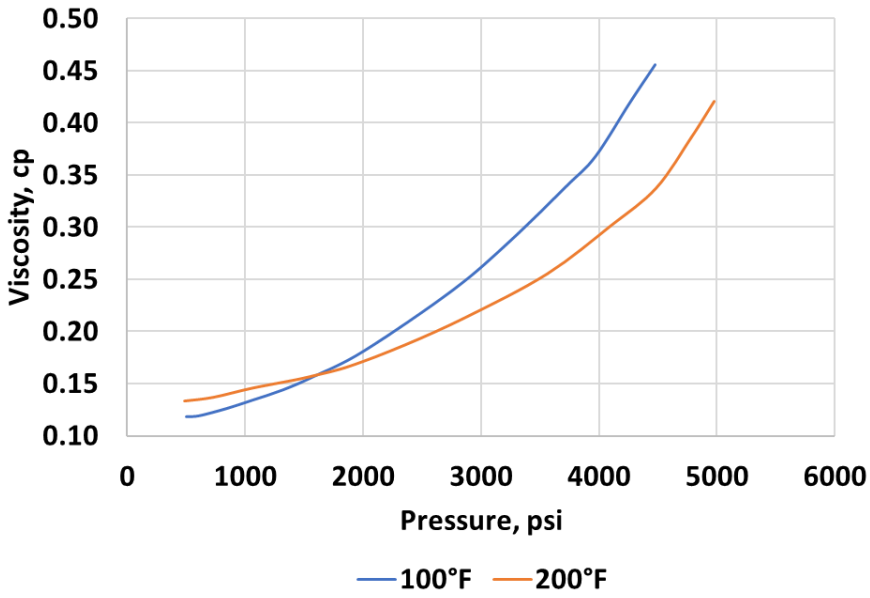

Figure 27. Variation of solution (Meramec oil-C1/C2(72/28) gas) viscosity as a function of pressure and temperature (from PVTSim software)